

Monte Carlo Simulation of Ion Implantation in Silicon-Germanium Alloys

R. Wittmann, A. Hössinger, and S. Selberherr

Institute for Microelectronics, TU Vienna
Gußhausstraße 27–29, A-1040 Wien, Austria
Email: Wittmann@iue.tuwien.ac.at

Abstract

We have extended our Monte Carlo ion implantation simulator for $\text{Si}_{1-x}\text{Ge}_x$ targets in order to analyze the applicability for advanced CMOS devices. The penetration depth of ion implanted dopants in relaxed SiGe is significantly reduced compared to pure silicon due to the larger nuclear and electronic stopping power. The successful calibration for the simulation of arsenic and boron implantations in $\text{Si}_{1-x}\text{Ge}_x$ with different germanium fraction x is demonstrated by comparing the predicted doping profiles with SIMS measurements. A shift towards shallower profiles with increasing germanium content was found in a non-linear manner. Finally, the simulation result of source/drain implants for a MOSFET structure on a SiGe substrate is presented.

1 Introduction

Strained silicon/relaxed SiGe CMOS devices have significant performance enhancements compared to pure silicon devices. The silicon-germanium (SiGe) material technology offers the possibility of bandgap engineering, enhanced carrier mobility, and a higher dopant solubility. The depth of source/drain junctions in $\text{Si}_{1-x}\text{Ge}_x$ can be significantly reduced with the increase of the germanium content x at a given implantation energy. In this paper we analyze the implantation of arsenic as an n-type and boron as a p-type dopant in crystalline SiGe with different composition. All Monte Carlo simulation experiments were performed with the object-oriented, multi-dimensional ion implantation simulator MCIMPL-II [1], [2]. The simulator is based on a binary collision approximation (BCA) and cells arranged on an ortho-grid are used to count the number of implanted ions and of generated point-defects.

2 Modelling of the SiGe Crystal

The lattice parameter $a(x)$ of $\text{Si}_{1-x}\text{Ge}_x$ crystals depends on the germanium fraction x and can be calculated by the quadratic expression (1) which approximates experimental data with a maximum deviation of about 10^{-3} Å [3].

$$a(x) = 0.02733 x^2 + 0.1992 x + 5.431 \quad (\text{Å}) \quad (1)$$

While the ion moves through the target, a local crystal model is built up around the actual ion position for searching the next collision partner (Figure 1). The selection of the target atom species in the crystal model is defined by probability x for germanium and $1 - x$ for silicon, respectively.

3 Nuclear and Electronic Stopping Power

The total stopping process of the ions in the target solid is modeled as a sequence of alternating nuclear and electronic stopping processes. A scattering angle ϑ results from a nuclear collision event and can be calculated by relation (2) which depends on the scattering angle Θ in the center-of-mass coordinate system, on the mass M_1 of the ion, and on the mass M_2 of the involved atomic nucleus of the target [4].

$$\tan \vartheta = \frac{\sin \Theta}{\frac{M_1}{M_2} + \cos \Theta} \quad (2)$$

From (2) it can be derived that if the ion is heavier than the target atom ($M_1 > M_2$) then a maximal scattering angle $\vartheta_{\max} < 90^\circ$ exists according to (3).

$$\sin \vartheta_{\max} = \frac{M_2}{M_1} \quad (3)$$

For instance, if an arsenic ion hits a silicon atom then $\vartheta_{\max} = 22^\circ$, and if the arsenic ion hits the heavier germanium atom then a larger maximal scattering angle $\vartheta_{\max} = 69^\circ$ is possible. Due to the fact that the angles of subsequent collisions have to be added up for a turn around from the incident direction, the backscattering probability for the dopant atoms increases with the germanium content in SiGe.

The electronic stopping process is calculated by using the Hobler model which extends the Lindhard electronic stopping model (amorphous model) to crystalline silicon [5]. SiGe has a larger electronic stopping power than silicon, which is caused by the higher electron density of SiGe due to the electron-rich germanium atom.

4 Arsenic and Boron Implantation in SiGe

The Monte Carlo ion implantation simulator has been extended from crystalline silicon to $\text{Si}_{1-x}\text{Ge}_x$ targets. The calibration of the empirical electronic stopping model was performed by just arranging the Lindhard correction parameter k as a linearly rising function of the germanium fraction x . For the other three parameters of the model the values from crystalline silicon could be applied. The parameter $k_{\text{As}}(x)$ for arsenic is defined by equation (4) and it could be verified from pure silicon up to a germanium content of 50% by comparison with SIMS measurements (Figure 2).

$$k_{\text{As}}(x) = 1.132 + 1.736 x \quad (4)$$

Figure 2 shows the simulated and experimental doping profiles of arsenic implantations into $\text{Si}_{1-x}\text{Ge}_x$ layers with a thickness of 150 nm on a silicon substrate. All implantations were simulated with an energy of 60 keV, a dose of 10^{11} cm^{-2} , a tilt of 7° , and a twist of 15° . Two effects can be observed in this figure. Firstly, with increasing germanium fraction, there is a shift towards shallower arsenic profiles. Secondly, the germanium content produces a stronger decline of the arsenic concentration compared to silicon. It has been pointed out by (3) that the heavier germanium atom produces an increased backscattering probability for the dopant atoms. Additionally the electronic stopping power of $\text{Si}_{1-x}\text{Ge}_x$ increases with the germanium fraction x and thereby causes a stronger decline of the concentration profiles especially in the tail region.

Figure 3 presents simulated arsenic profiles resulting from an implantation with low energy and high dose. It again demonstrates the effect of the germanium content which facilitates the forming of shallow junctions but the trend to shallower profiles is non-linear. For instance, the difference between $x = 0$ and $x = 0.25$ profiles is larger than the difference between $x = 0.5$ and $x = 0.75$ profiles. All implantations were performed with an energy of 15 keV, a dose of 10^{15} cm^{-2} , a tilt of 7° , and a twist of 22° . For the calibration of boron implantations in $\text{Si}_{1-x}\text{Ge}_x$ a linearly rising function for the parameter $k_B(x)$ depending on x according to (5) was used.

$$k_B(x) = 1.75 + 0.75x \quad (5)$$

Figure 4 shows the simulated and experimental doping profiles of boron implantations into a $\text{Si}_{1-x}\text{Ge}_x$ layer with a thickness of almost 330 nm on a silicon substrate. All implantations were simulated with an energy of 50 keV, a dose of 10^{15} cm^{-2} , and a tilt of 7° . Figure 4 points out that boron implants in $\text{Si}_{1-x}\text{Ge}_x$ show qualitatively the same characteristics as arsenic implants. Figure 5 compares simulated boron profiles in targets with different germanium content. All these simulations were performed with an energy of 5 keV, a dose of 10^{15} cm^{-2} , and a tilt of 7° .

5 Two-Dimensional MOSFET Application

The excellent properties of $\text{Si}_{1-x}\text{Ge}_x$ alloys for forming shallow vertical junctions are demonstrated on a 100 nm gate n-MOSFET structure on a $\text{Si}_{0.75}\text{Ge}_{0.25}$ substrate. Using scaling considerations, a source/drain vertical junction depth of 40 nm to 80 nm is recommended for processing of such a MOS transistor. Figure 6 shows the Monte Carlo arsenic source/drain and extension implants for such a transistor. The simulation was performed with 2.000.000 simulated ions per implantation step. In the first implantation step the source/drain extensions were formed with an energy of 15 keV, a dose of $4 \cdot 10^{13} \text{ cm}^{-2}$, a tilt of 7° , and a twist of 22° . The source/drain implantation step was performed with an energy of 45 keV and a dose of $2 \cdot 10^{15} \text{ cm}^{-2}$. Although a relatively large energy of 45 keV was used, the required junction depth was met.

Acknowledgments

I am indebted to Dr. Pauli Laitinen and Prof. Dr. Herbert Hutter for providing SIMS measurement data and background information about the experiments. This work has partly been supported by the Austrian Program for Advanced Research (APART) from the Austrian Academy of Science.

References

- [1] G. Hobler and S. Selberherr, IEEE Transactions on CAD **8**, 450 (1989).
- [2] R. Wittmann, A. Hössinger, and S. Selberherr, Proceedings ESS 2003 **1**, 35 (2003).
- [3] E. Kasper and K. Lyutovich, *Properties of Silicon Germanium and SiGe:Carbon* (INSPEC, London, United Kingdom, 1999).
- [4] J. Ziegler, *Ion Implantation Science and Technology* (Ion Implantation Technology Co., New York, 1996).
- [5] G. Hobler and H. Pötzl, Proceedings Mat.Res.Soc.Symp. **279**, 165 (1993).

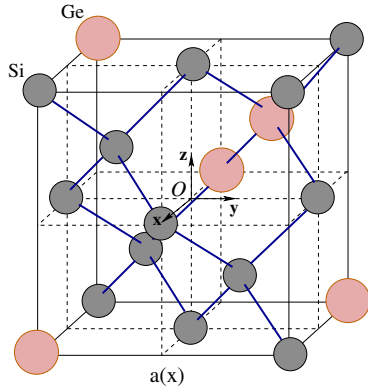


Figure 1: $\text{Si}_{1-x}\text{Ge}_x$ crystal simulation model

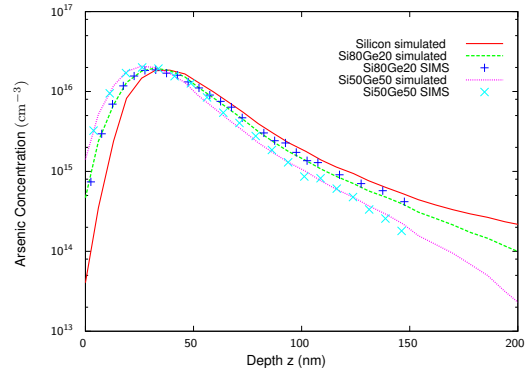


Figure 2: Simulated 60 keV arsenic implantations in $\text{Si}_{1-x}\text{Ge}_x$ with $x = 0, 20\%, 50\%$ compared to SIMS measurements

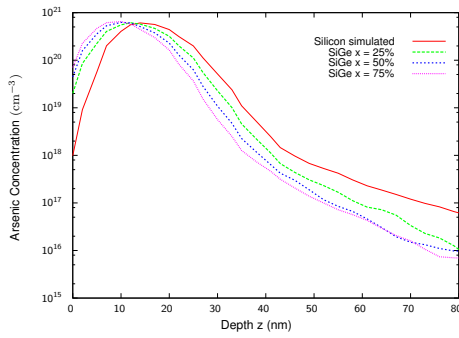


Figure 3: Simulated 15 keV arsenic profiles in $\text{Si}_{1-x}\text{Ge}_x$ with $x = 0, 25\%, 50\%, 75\%$

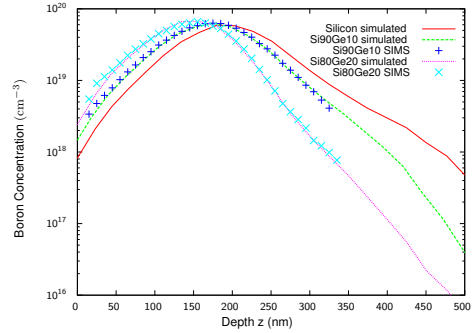


Figure 4: Simulated 50 keV boron implantations in $\text{Si}_{1-x}\text{Ge}_x$ with $x = 0, 10\%, 20\%$ compared to SIMS measurements

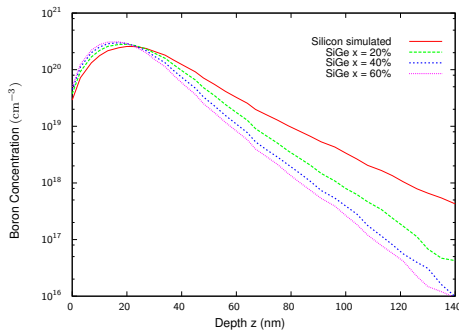


Figure 5: Simulated 5 keV boron profiles in $\text{Si}_{1-x}\text{Ge}_x$ with $x = 0, 20\%, 40\%, 60\%$

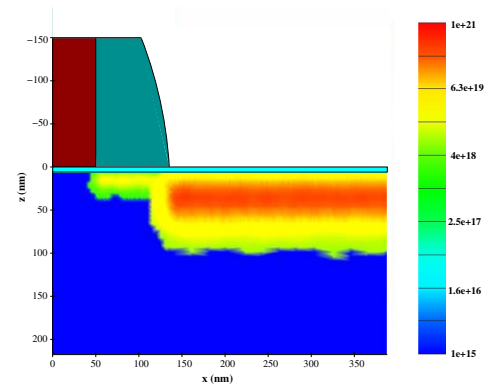


Figure 6: Simulated cross-section of an n-MOSFET structure on a $\text{Si}_{0.75}\text{Ge}_{0.25}$ substrate